



# Acoustic and ultrasonographic characterization of polychloroprene, beeswax, and carbomer-gel to mimic soft-tissue for diagnostic ultrasound

Debjani Phani<sup>1,2</sup> · Rajasekhar Konduru Varadarajulu<sup>3</sup> · Anjali Thomas<sup>4</sup> · Raghukumar Paramu<sup>1</sup> · M. Suheshkumar Singh<sup>4</sup> · V. S. Shaiju<sup>1</sup> · Venugopal Muraleedharan<sup>5</sup> · Raghuram Kesavan Nair<sup>1</sup>

Received: 9 April 2020 / Accepted: 9 August 2020 / Published online: 18 August 2020

© Australasian College of Physical Scientists and Engineers in Medicine 2020

## Abstract

Materials with acoustic properties similar to soft-tissue are essential as tissue-mimicking materials (TMMs) for diagnostic ultrasound (US). The velocity ( $c_{us}$ ), acoustic impedance (AI) and attenuation coefficient of US ( $\mu$ ) in a material collectively define its acoustic property. In this work, the acoustic properties of polychloroprene rubber, beeswax, and Carbomer-gel are determined. The pulse-echo technique is used to estimate  $c_{us}$  and  $\mu$ . The product of a sample density ( $\rho$ ) and  $c_{us}$  gives its AI. Using a reference based on the *International Commission on Radiation Units and Measurements Report-61, Tissue Substitutes, Phantoms and Computational Modelling in Medical Ultrasound*, the results are evaluated. The acceptance criteria are  $1.043 \pm 0.021 \text{ g/cm}^3$  ( $\rho$ ),  $1561 \pm 31.22 \text{ m/s}$  ( $c_{us}$ ),  $1.63 \pm 0.065 \text{ MRayls}$  (AI) and  $\mu$  within 0.5–0.7 dB/cm/MHz. Sample computerized tomography (CT) and US scanning are performed to evaluate their similarities (contrast and speckle pattern) with respective images of the human liver (a clinical soft-tissue). The average errors in measuring  $c_{us}$  and  $\mu$  were 0.14% and 1.2% respectively. From the present findings, acoustic properties of polychloroprene and beeswax are unacceptable. However, the results of Carbomer-gel  $\rho = 1.03 \text{ g/cm}^3$ ,  $c_{us} = 1567 \text{ m/s}$ ,  $\text{AI} = 1.61 \text{ MRayls}$  are satisfactory and  $\mu = 0.73 \text{ dB/cm/MHz}$ , is higher than the reference (4.3%). Carbomer-gel could produce CT and US images, efficiently mimicking the respective liver images. Carbomer-gel containing 95% water is a low-cost material with a simple formulation. Present results suggest, Carbomer-gel mimics soft-tissue and can be used as a TMM for diagnostic US.

**Keywords** Acoustic quantities · Tissue-mimicking materials · Measurement of ultrasound velocity · Ultrasound image analysis · Carbomer gel

✉ Debjani Phani  
debjaniaphani@gmail.com

Rajasekhar Konduru Varadarajulu  
roshoraju@gmail.com

Anjali Thomas  
anjaliathomas16@iisertvm.ac.in

Raghukumar Paramu  
raghu.rcc@gmail.com

M. Suheshkumar Singh  
suhesh.kumar@iisertvm.ac.in

V. S. Shaiju  
shaijuvs@gmail.com

Venugopal Muraleedharan  
drvenurcc@gmail.com

Raghuram Kesavan Nair  
raghurkn@gmail.com

- 1 Department of Radiation Physics, Regional Cancer Centre, Thiruvananthapuram, Kerala 695011, India
- 2 Meenakshi Academy of Higher Education and Research, Chennai, Tamilnadu 600 078, India
- 3 Department of Radio Diagnosis, Meenakshi Medical College Hospital & Research Institute, Chennai, Tamilnadu 631 552, India
- 4 School of Physics, Indian Institute of Science Education and Research Thiruvananthapuram (IISER-TVM), Vithura, Thiruvananthapuram, Kerala 695551, India
- 5 Department of Radio Diagnosis, Regional Cancer Centre, Thiruvananthapuram, Kerala 695011, India

## Introduction

An ultrasound (US) phantom is essential for quality control and periodic evaluation of diagnostic US equipment. These phantoms consist of tissue-mimicking materials (TMMs) that can produce US images equivalent to a clinical setup. Commercial phantoms are highly expensive. Unfortunately, in many countries providing an US scanning facility to every patient is a problem and implementing a periodic quality assurance program using a phantom poses a financial burden. This often results in disregarding quality assurance for US scanners. Indigenous phantoms mostly developed for clinical training, have used biodegradable TMMs like gelatine and agar [1–3]. An agar phantom can last around 2.5 years with preservatives and maintaining the storage conditions [4]. However, for a quality assurance phantom, the TMM should have a longer shelf-life, preferably 5 to 10 years. Secondly, to mimic a tissue for the US, this material should have acoustic properties, similar to the tissue for the range of frequencies (~3–25 MHz) used during US imaging. To explore low-cost, stable TMMs in this work, we aim to experimentally determine the acoustic properties of three different materials. The acoustic property of a material is defined by a set of physical parameters, most critical are the velocity of US ( $c_{us}$ ), acoustic impedance (AI), attenuation coefficient ( $\mu$ ), back-scattering coefficient, and the non-linearity parameter [5]. Ideally, a TMM should have the  $c_{us}$  equal to 1540 m/s ( $\pm 10$  m/s), AI of  $1.6 \times 10^6$  Rayls, and  $\mu$  in the range of 0.5–0.7 dB/cm/MHz, for frequencies ranging from 2 to 15 MHz, with a linear response of attenuation to frequency [6, 7]. A material with similar values will ensure image resolution, contrast and depth of penetration equivalent to soft-tissue during US imaging. Moreover, the US images of these samples were also analyzed for their ability to mimic the human liver (a homogeneous soft-tissue).

The  $c_{us}$ , AI, and  $\mu$  in polychloroprene (neoprene) rubber, beeswax, and carbomer-gel (*C-gel*) were determined. The present samples were chosen for their stability, low-cost, and/or the  $c_{us}$  close to 1540 m/s. ATS–Laboratories (Bridgeport, CT), presently CIRS Inc. (Norfolk, VA) uses urethane rubber ( $c_{us} \sim 1450$  m/s, desired  $> 5\%$ ) as TMM in an US phantom. But, polychloroprene was selected in this study because of its reported  $c_{us} \sim 1600$  m/s (desired  $< 3.9\%$ ) [8]. Furthermore, the hardness for a soft rubber is designated by its shore-A value which is experimentally determined using the American Society for Testing and Materials (ASTM) Standard D-2240 [9]. The present sample of polychloroprene was prepared to have the shore-A value of 50 (polychloroprene-50). The second sample was a block of beeswax. Finally, a water-based gel was chosen. Water is universally available and it

can transmit US signals. To increase the viscosity of water carbomer-gel (*C-gel*) was prepared. This *C-gel* contained water (95%) and carbomer-940 powder (5%). Carbomers are synthetic high molecular weight polymers of acrylic acid (polyacrylic acid) commonly used in pharmacology [10, 11]. Carbomer-940 can produce highly viscous stable gels that do not flow at normal room temperature.

Mass densities ( $\rho$ ) of the prepared samples were determined from the computerized tomography (CT) scan and also using Archimedes Principle. The  $c_{us}$  in the test samples was measured using the time of flight method and the AI was then calculated from the product of  $\rho$  and  $c_{us}$ . Finally,  $\mu$  (dB/MHz/cm) of each sample was measured using Beer-Lambert's Law [12, 13]. Furthermore, the CT and US scan images of each sample were compared with the respective images of the liver for similarity in image contrast and echogenicity. The results of the acoustic properties were compared with the values given in Table 1.

Table 1 presents the average value of acoustic properties for soft-tissues obtained from the International Commission on Radiation Units and Measurements (ICRU) Report 61 and a reference by Duck reported by Mast et al. [14–16]. Here, the AI was obtained from the product of  $\rho$  and  $c_{us}$ . This table was used as a benchmark in the current work, to assess the acoustic properties of the present samples. In an US image, the tissues of muscles, tendons, ligaments, fascia, fat, fibrous tissue, synovial membranes, nerves, and blood vessels are known as soft-tissues [17]. The reported reference values by T.D. Mast show the  $c_{us}$ ,  $\rho$ , and  $\mu$  were different in these tissues [14]. The percentage variations of  $c_{us}$  and  $\rho$  were 10% and 16.3% respectively in this data. Therefore, it is practically reasonable to allow an acceptable range of  $\pm 2\%$  for the acoustic properties.

Based on these criteria in this study, the following conditions are set for a material to qualify as a TMM for diagnostic US.

- (i) The value of  $\rho$  should be  $1.043 \pm 0.021$  g/cm<sup>3</sup>,  $c_{us}$   $1561 \pm 31.22$  m/s and AI  $1.63 \pm 0.07$  MRayls in a sample. These ranges allow the  $\rho$  and  $c_{us}$  to vary within  $\pm 2\%$  (refer to Table 1) and AI within  $\pm 4\%$ .

**Table 1** Benchmark to characterize the acoustic properties of the samples

| $\rho$ (g/cm <sup>3</sup> ) | $c_{us}$ (m/s) | AI (MRayls) | $\mu$ (dB/cm/MHz) |
|-----------------------------|----------------|-------------|-------------------|
| 1.043                       | 1561           | 1.63        | 0.5–0.7           |

*Source:* Empirical relationships between acoustic parameters in human soft-tissues, T.D. Mast [14] derived from ICRU Report -61 and Duck F.A. [14–16]. The table presents the reference values of density ( $\rho$ ), velocity of ultrasound ( $c_{us}$ ), acoustic impedance (AI), and attenuation coefficient ( $\mu$ ) for human soft-tissues

Besides, the value of  $\mu$  should be in the range 0.5–0.7 dB/cm/MHz.

- (ii) A sample should produce a homogeneous CT contrast similar to the CT of normal human liver. Moreover, the US image of a sample should mimic the speckle pattern of liver US image, according to the recommendations of ICRU-61 [15].

## Materials and method

The steps involved in determining the acoustic properties of the samples are illustrated in Fig. 1.

### Sample preparation

#### Polychloroprene (neoprene) rubber

Polychloroprene-50 was compounded by a professional rubber products manufacturer. A cylindrical stainless-steel die was cast for the required dimension of polychloroprene (diameter = 5 cm and height = 7 cm).

**Ingredients** Raw polychloroprene (Skyprene® B-30, 100 phr), Magnesium Oxide (MgO, 1 phr), Antioxidant (AO45, 2 phr), Ultraflow (UF500, 2 phr), Carbon Black (HAF 330, 25 phr), Precipitated Silica (40 phr), Naphthalene Oil (N-oil,

Elasto 541, 3 phr), Zinc Oxide (ZnO, 4 phr), Ethylene Thiourea (NA22, 2 phr), and Tetra Methylthiuram Disulphide (TMTD, 0.6 phr).

**Mixing** Polychloroprene rubber was masticated in a rubber mill for 10 min, and then MgO was added to the rolling band and mixed. UF500 and AO45 were added one at a time and mixed in between. To this HAF330, precipitated silica and N-oil were added across the mill and again mixed for 10 min. Finally, ZnO, NA22, and TMTD were added. The compound was thoroughly mixed to ensure a homogeneous mix. The dosage of carbon black (HAF 330) decides the shore value of rubber and antioxidants ensure good ageing properties and stability.

**Molding** The rubber sample was moulded in a hydraulic press. The prepared stainless-steel die was preheated, compounded mix was poured, and appropriate feed weight was placed onto it in a press of dimension  $50.8 \times 55.9 \times 45.7 \text{ cm}^3$ . After setting the curing parameters (temperature = 423.15 K and pressure = 15 MPa) the press was closed. The product was taken out after 30 min. Figure 2a shows the prepared sample of polychloroprene.

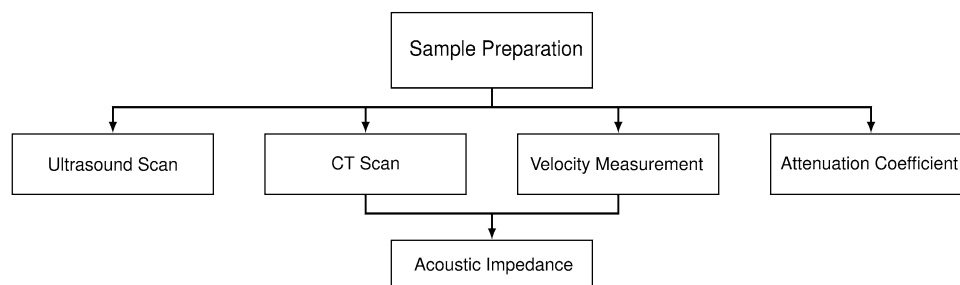
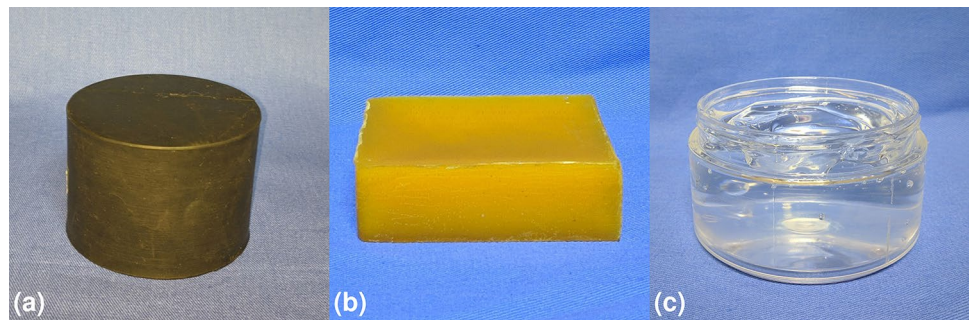


**Fig. 1** Steps involved in determining the acoustic properties- Prepared samples were imaged in a computerized tomography (CT) and an ultrasound scanner. The velocity and attenuation coefficient

of ultrasound were determined using the pulse-echo technique. The product of density (obtained from the CT) and velocity gave the acoustic impedance

**Fig. 2** Sample photographs: **a** the compounded polychloroprene (Shore-A value 50), **b** the block of beeswax, and **c** the prepared carbomer-gel at 26 °C



## Beeswax

Filtered beeswax blocks (Hill Dews™) were purchased. Using a heated stainless-steel needle a cavity (~8 mm depth) was made in the wax. This cavity was filled with water from a syringe and wax sealed. The excess water overflowed during sealing and ensured the cavity to be free from any air-pockets. The aim was to view this water-well in CT and US scans. The specimen of beeswax is shown in Fig. 2b.

## Carbomer gel

**Ingredients** Distilled water, ethanol (Merck CAS# 64-17-5), carbomer-940 powder (Carbogel®-940 Maruti Chemicals) and triethanolamine (Spectrum Chemicals).

**Procedure** 100 ml of an ethanol–water mixture (70%) was taken in a beaker. While stirring on a magnetic stirrer carbomer-940 powder (5 g, 5% carbomer in the solution) was sifted into it. After thoroughly mixing, the solution was filtered into a jar preventing any lump. To these three drops of triethanolamine were added. The jar was closed and mixed vigorously forming a viscous gel. The prepared gel was then placed in a vessel containing deionized water for ~1 h under a reduced pressure (~0.5 atm). The air bubbles coalesced and pop out once reached near surface. This was then stored in a container. The prepared *C-gel* sample at 26 °C is shown in Fig. 2c.

## Computerized tomography and ultrasound scan

A 16-slice CT (Optima CT580 W) and US scanner (LOGIQ P5) from GE Healthcare were used to scan the samples. CT

was performed to ascertain the samples were free from air-pockets and obtain their densities. Exposure parameters of 120 kV, 277 mA, and a slice thickness of 0.63 mm were used during CT imaging. The CT DICOM (Digital Imaging and Communications in Medicine) images were then exported to the Eclipse™ v-13.6 (Varian Medical Systems, Palo Alto, CA) system. The Eclipse™ radiation therapy planning system was commissioned using a calibration curve of the Hounsfield Unit (from CT data) and material densities using a CT phantom (CATPHAN 500) with known in homogeneities [18, 19]. Eclipse™ could display the density on a CT image at any point of interest, using the *Physical Parameters Tool* in the *External Beam Planning Application*. The uncertainty in measuring  $\rho$  in the Eclipse™ system ( $\pm 0.36\%$ ) was determined from the deviation of the average value of  $\rho$  at 10 points in a region of interest in the CATPHAN CT image and the actual density of this region from the phantom data-sheet.

US scans were performed on the present samples using a 4C curvilinear probe (nominal frequency 4 MHz), having a footprint of  $18 \times 66$  mm, bandwidth 1.6–4.6 MHz and the gain ranging from 76–92 during imaging. The US scanning was carried out and evaluated by an experienced radiologist to establish the ability of a sample to mimic the speckle pattern obtained from the US imaging of the human liver.

## Ultrasound velocity measurement

The experimental set-up used for measuring the  $c_{us}$  and  $\mu$  is illustrated in Fig. 3a. The set-up used for the experiments shown in Fig. 3b, composed of a pulser-receiver (5073PR-40-P, Olympus, with pulse repetition frequency of 100 Hz, 25 MHz nominal frequency,

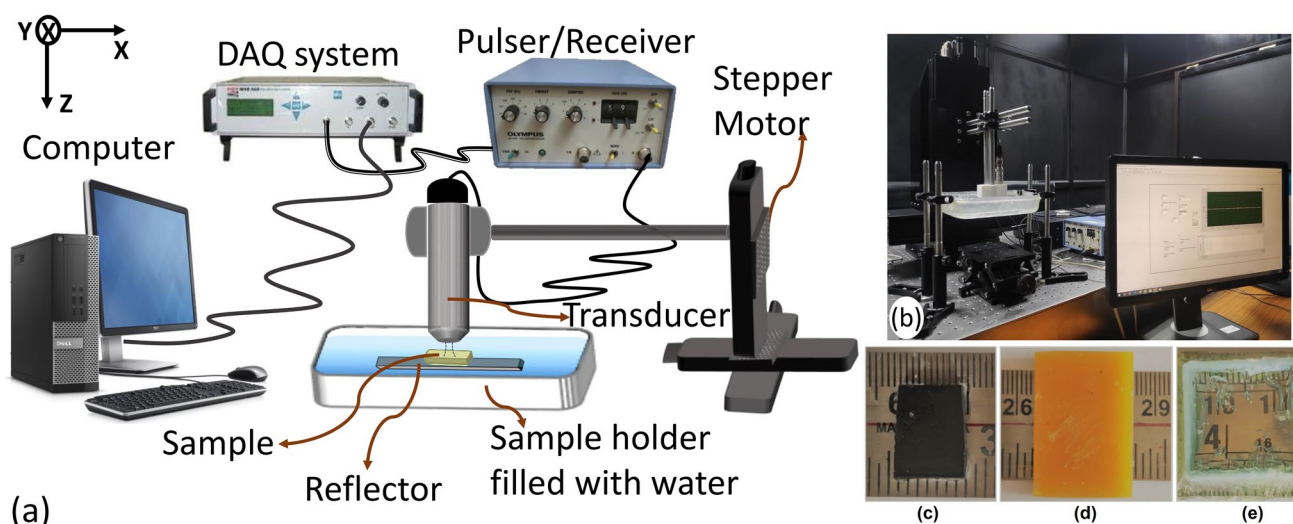


**Fig. 3** a Schematic representation of the experimental set-up to measure the ultrasound velocity and attenuation coefficient in a specimen. b Photograph of the experimental set-up. c–e Photographs of sample sections polychloroprene-50 (c), beeswax (d), and *C-gel* (e)



and pulse width ~ nano sec), a focusing US transducer (V 375—SU, Olympus with 19 mm focal length, focal spot size ~ 153  $\mu\text{m}$ , and focal zone length of 4 mm), a 3-Axis step-by-step motorized positioning system (Newmark NSC-G Series, Newmark Systems Inc.) and the data acquisition (DAQ) system (779745-02, NI PCI-5114). In time-sharing mode, the pulser-receiver also served as a sensor to receive electrical signals, corresponding to reflected acoustic pulses that could amplify weak signals (amplification ~ 39 dB). During the experiments, samples were mounted on an acoustic reflector (a stainless- steel plate) and fully immersed in a water bath (18 °C) along with the transducer surface for acoustic coupling. Samples were kept at the focal zone of the transducer for delivering maximum energy of acoustic signals and a train of acoustic pulses were delivered to the material. The acoustic echoes (A-line data) reflected from sample surfaces, were acquired by the DAQ system after amplification, at a sampling frequency of ~ 250 MHz. Figures 3c–e show the photographs of small sections of the samples polychloroprene-50 ( $10 \times 15 \times 1.93 \text{ mm}^3$  obtained by slicing the sample shown in Fig. 2a using a slow motorized saw), beeswax ( $20 \times 40 \times 2.64 \text{ mm}^3$ , prepared by melting and pouring the beeswax in a stainless-steel mould), and the C-gel ( $18 \times 18 \times 4 \text{ mm}^3$ , by taking a small quantity in a small glass container with open ends for measurements).

### Experimental procedure

To estimate the  $c_{us}$ , pulse-echo method was implemented. Incident US pulses reflected from the topmost (at time  $t_1$ ) and the distal surface of the sample (at time  $t_2$ ) were obtained. The A-line data recorded in the experimental system for polychloroprene-50 is depicted in Fig. 4. We performed envelope detection of A-line data (representing variation of reflected US-signal against  $t$ ) employing Hilbert Transform (in MATLAB) and time points corresponding to the two local maxima (shown in the inset of Fig. 4) are determined as  $t_1$  and  $t_2$ . Data were post-processed and the  $c_{us}$  were measured using the time-of-flight equation. The time interval  $\Delta t$  ( $\Delta t = t_2 - t_1$ ) was the time taken by the acoustic pulses to travel two times across the thickness ( $d$ ) of the sample. So, in time  $\Delta t$ , the pulses traverse the sample with an effective thickness  $d_{\text{eff}}$  ( $d_{\text{eff}} = 2d$ ).

Using the expression,  $d_{\text{eff}} = c_{us} \times \Delta t$ , the  $c_{us}$  of the samples were obtained using the equation

$$c_{us} = d_{\text{eff}} / \Delta t$$

For each sample, the experiment was repeated ten times and data were averaged.

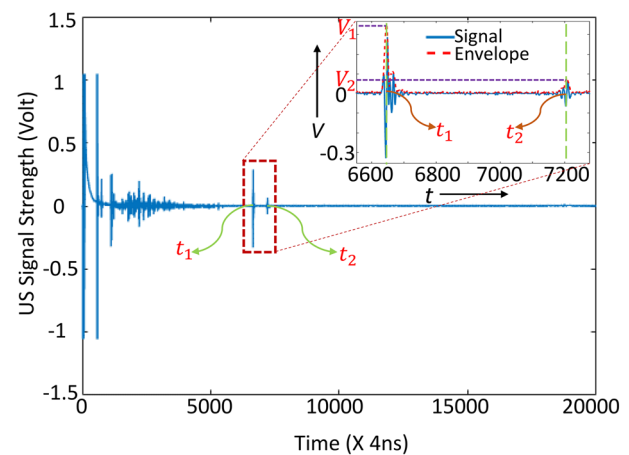


**Fig. 4** A-line plot showing variation of reflected ultrasound (US) signal strength against time ( $t$ ) for the polychloroprene-50 sample (thickness ~ 1.93 mm). The figure shows the reflected signals from the proximal ( $V_1$ ) and distal ( $V_2$ ) surfaces of the specimen, corresponding to the times  $t_1$  and  $t_2$  respectively. The inset depicts an enlarged view of the data within the dotted rectangular box. The inset figure displays envelope detection of the curve (shown by red dotted curve) and two local maxima (marked by two vertical green dotted lines) to determine  $t_1$  and  $t_2$

### Estimation of acoustic impedance

The product of  $\rho$  (from the Eclipse™) and experimentally determined  $c_{us}$  in a sample gave the AI ( $\text{kg/m}^2/\text{s}$  or Rayls). This was obtained for all the samples.

### Attenuation coefficient measurement

The  $\mu$  for the present samples were measured using the setup shown in Fig. 3a. Propagation of US waves in a material obeys Beer-Lambert's Law [12]. This law states that the intensity of acoustic waves decays exponentially while propagating through a material.

$$I = I_0 \times e^{-\mu \times d_{\text{eff}}}$$

Here,  $I_0$  and  $I$  are the intensity of the incident wave and the intensity after traversing through an effective distance  $d_{\text{eff}}$  ( $d_{\text{eff}} = 2d$ ) in the sample respectively and " $\mu$ " denotes the attenuation coefficient.

From wave theory, the reflection coefficient ( $R$ ) of propagating waves at any interface separating two media of acoustic impedances ( $AI_1$  and  $AI_2$ ) is given by  $R = [(AI_2 - AI_1) / (AI_2 + AI_1)]^2$  (for normal incidence, as it is in our case) [12]. From the measurement of reflection coefficient ( $R$ ), one can estimate the intensity or power of incident waves (acoustic or optical) using the relationship,  $R = I_{\text{refl}} / I_{\text{inc}}$  (where  $I_{\text{refl}}$  and  $I_{\text{inc}}$  are intensities of reflected and incident waves). Again,

we can obtain the effective acoustic energy that is transmitting through the topmost surface of the sample as

$$I_{trans}^{(top)} = T \times I_{inc}^{(top)} = I_{inc}^{(top)}(1 - R^{(top)}) = \frac{I_{refl}^{(top)}}{R^{(top)}}(1 - R^{(top)})$$

Here, “T” is the transmission coefficient which is related to “R” by  $T + R = 1$ .

Similarly, effective acoustic intensity arriving at the distal surface can be estimated by

$$I_{inc}^{(dist)} = \frac{I_{refl}^{(dist)}}{R^{(dist)}}$$

On the other hand, the strength of acoustic signals ( $V_1$  and  $V_2$ ) corresponding to pulses reflected from the sample topmost surface and the distal surface/reflector, as they were detected by an acoustic sensor (ultrasound transducer, in our case) kept in sample boundary (shown in inset of Fig. 4), were measured as local maxima (corresponding to  $t_1$  and  $t_2$ ) of the demodulated time-resolved signal (represented with the red dotted curve in inset of Fig. 4) obtained by Hilbert transform in time-resolved acoustic signal (refer to Fig. 4).

We know that the electrical voltage (V), which is obtained as output reading from the acoustic sensor, is related to acoustic pressure intensity (I) by  $I = \beta V$  [20, 21] (where,  $\beta$  is the coupling constant being characterized by electrical and physical parameter of the transducer), i.e., under the similar experimental conditions for measuring  $V_1$  and  $V_2$  (as it is in the case of our present study),  $\frac{V_1}{V_2} = \frac{I_{refl}^{(top)}}{I_{refl}^{(dist)}}$

Now, from the experimental measurements of  $V_1$  and  $V_2$  with the given  $R^{(top)}$  and  $R^{(dist)}$ , we can estimate the acoustic attenuation coefficient,  $\mu$  (in dB/cm) using the Beer-Lambert’s law as

$$\mu = \frac{10}{2d} \log \frac{\frac{V_1}{R^{(top)}}(1 - R^{(top)})}{\frac{V_2}{R^{(dist)}}} \text{ in dB/cm}$$

This equation takes into account the loss in signal strengths at the interfaces separating two different media, with the loss being characterized by the reflection coefficient (R). In order to estimate  $\mu$  from the experimental measurements of  $V_1$  and  $V_2$ , we determined acoustic reflection coefficients (R) for every interface from the AI of media taking the product of a sample  $\rho$  and  $c_{us}$ . We found the values of AI equal to 2.47 MRayl, 2.23 MRayl, 1.614 MRayl, 1.5 MRayl and 45 MRayl for polychloroprene-50, beeswax, *C-gel*, water and steel respectively [22]. The value of R obtained using these values of AI were 0.0600 (water- polychloroprene 50), 0.8024 (polychloroprene 50-steel), 0.0013 (water- *C-gel*), 0.8664 (*C-gel*-steel), 0.0384 (water- beeswax), 0.82 (beeswax -steel).

Attenuation of ultrasonic waves (expressed in dB) can be approximated to a linear dependence on frequency (expressed in MHz) (0.5 dB/cm/MHz, for soft tissues) [12, 13]. Therefore, under a linear approximation, the estimated value of  $\mu$  was divided by the operating frequency of ultrasound transducer (25 MHz) to obtain the value of  $\mu$  in dB/cm/MHz.

## Results

Figure 5 presents the CT and US images of the prepared samples and that of the human liver.

Figure 5a–c show the CT images of the polychloroprene-50, beeswax, and *C-gel*. The respective US images are shown in Fig. 5e–g. These images are compared to the benchmark CT and US scans of human liver shown in Fig. 5d and h.

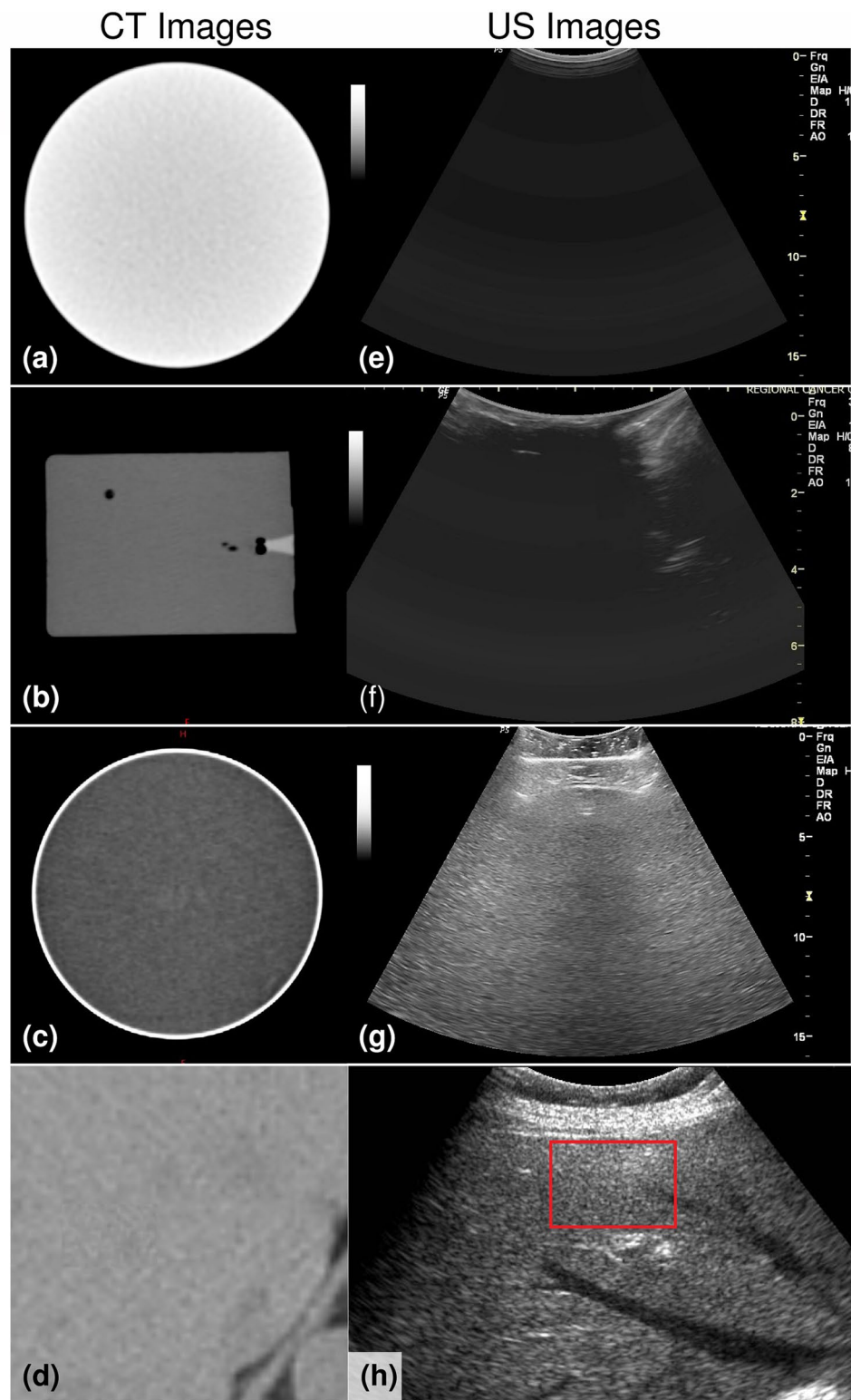
Table 2 presents the densities of the samples measured from the Eclipse™ system and their physically measured densities. Based on the evaluation of the radiologist, this table also reports the performance of all sample images (CT and US) when compared to the respective liver scans. The CT images of the liver/soft-tissue and the test material shall be similar in image contrast for the CT results to be acceptable. The contrast of a subject in a CT image is determined by the difference in the Linear Attenuation Coefficient of adjacent objects for photons. Moreover, this coefficient defined by the fraction of attenuated incident photons in a monoenergetic beam per unit thickness of a material, increases with increasing physical density of the subject. Therefore, the outcome of a sample CT can also be determined from its “ $\rho$ ”. But, performing a CT scan is essential to know the construction of a sample. In both the (CT and US) scans the samples are homogenous, except for few small air-pockets in the beeswax sample caused while forming the water-well see Fig. 5b. Sample homogeneity is crucial for the acoustic property ( $\rho$ ,  $c_{us}$ , AI and  $\mu$ ) to be uniform in a sample. Moreover, for the US image of a material to be acceptable, it shall produce speckle patterns similar to soft-tissue/liver during US imaging.

The ( $\rho$ ) of polychloroprene-50 (1.45 g/cm<sup>3</sup>) is the highest among the present samples followed by *C-gel* (1.03 g/cm<sup>3</sup>) and beeswax (0.96 g/cm<sup>3</sup>). The *C-gel* produces image that could closely mimic the CT image contrast and the speckle pattern (US echogenicity) in the respective liver images. Therefore, the CT and US images of *C-gel* are acceptable.

Table 3 lists the experimentally determined acoustic properties for the present samples. This table also gives the percentage difference (% deviation) of each parameter compared to its corresponding value in benchmark Table 1.

The uncertainty in  $c_{us}$  measurements calculated using the values given in Table 3 is 0.05%, 0.10% and 0.28% for

**Fig. 5** Computerized Tomography and Ultrasound Images of the Samples. **a–c** show the CT images of polychloroprene-50, beeswax and the carbomer-gel respectively. **e–g** show their respective US images. **d** and **h** CT and US of human liver, are presented here as the benchmark images representing soft-tissue (the box shows the region of interest to compare in a sample US image)



polychloroprene-50, beeswax, and C-gel respectively. Similarly, the uncertainty in measurement of  $\mu$  in these samples is 1.05% 0.7% and 1.8%, in the same order. The errors in the measurement (for  $c_{us}$  and  $\mu$ ) are low indicating a

high accuracy in the measurements. This uncertainty associated with the measurement of the acoustic parameters (from ten separate experimental data sets) may be a result of experimental error and/or sample preparation.

**Table 2** Results from the CT and US scans of the samples

| Sample             | $\rho$ (g/cm <sup>3</sup> ) |                       | Acceptable (Yes/No) |          |
|--------------------|-----------------------------|-----------------------|---------------------|----------|
|                    | Ratio <sup>†</sup>          | Eclipse <sup>TM</sup> | CT-Image            | US-Image |
| Polychloroprene-50 | 1.38                        | 1.45                  | No                  | No       |
| Beeswax            | 0.98                        | 0.96                  | Yes                 | No       |
| C-gel              | 1.01                        | 1.03                  | Yes                 | Yes      |

Sample densities ( $\rho$ ) from the ratio and Eclipse<sup>TM</sup> system are produced. This table mentions if an image mimics the contrast (in CT) and speckle patterns (in US) in the corresponding liver images

<sup>†</sup>Physically measured ratio of mass to volume of the samples obtained using Archimedes Principle

## Discussions

The acoustic properties of soft-tissue based on ICRU Report-61 are set as the benchmark in the current work [15]. Then, acoustic properties of the three samples are determined and the percentage difference of a sample result from the reference value is obtained. Furthermore, the sample images (CT and US) were compared with the respective liver images to evaluate their similarity in image contrast (in CT image) and ability to produce speckled pattern (in US image).

### Polychloroprene (neoprene)

From Tables 2 and 3 the  $\rho$  of polychloroprene-50 (1.45 g/cm<sup>3</sup>) is higher than the desired density value (desirable < 39%) and unacceptable. This is also confirmed from Fig. 5a, where the CT image of polychloroprene shows a high-density material compared to the human liver (see Fig. 5d). Previous studies have found the  $\rho$  in polychloroprene increases with the shore-A value [8, 23]. Therefore,  $\rho$  of the present polychloroprene may decrease if its shore-A value is reduced from the present value. Furthermore, the US image of polychloroprene is anechoic, as shown in

Fig. 5e. Scattering is critical for producing echo details in B-mode images. This acoustic scattering caused by the inhomogeneity in a medium is a result of multiple reflections in a small volume from the changes in local  $c_{us}$  and/or  $\rho$ . Absence of scattering prevents image formation during an US procedure. Similarly, in the case of polychloroprene, the anechoic image can be a consequence of the material lacking sources of acoustic scattering.

Table 3 shows the  $c_{us}$  in polychloroprene 1706 m/s is higher by 9.3% from the required velocity 1561 m/s. Garu et al. found the  $c_{us}$  in polychloroprene -50 to be 1620 m/s in their samples. Our  $c_{us}$  in polychloroprene-50 is higher by 86 m/s (5.3%) from this data. It has been reported that the type of carbon black used for compounding polychloroprene significantly affects its acoustic parameters. Following the recipe and procedure meticulously is also crucial, as these results are sensitive to the compounding process [23]. In our sample, the AI 2.47 MRayls is higher by 51.5%. This large deviation in AI is primarily caused by the variation in  $\rho$  (39%) from the desired value 1.043 g/cm<sup>3</sup> (refer to Table 1). Moreover, the value of  $\mu$  in polychloroprene 1.80 dB/cm/MHz does not lie within the desirable range 0.5–0.7 dB/cm/MHz and is therefore unacceptable. There is a significant deviation in the CT and US images of polychloroprene and the liver in Fig. 5. Owing to the results of the  $\rho$ ,  $c_{us}$ , AI and  $\mu$  that do not satisfy our acceptance criteria in “Introduction” polychloroprene-50 does not qualify as a TMM for diagnostic US. Although the results of the present rubber sample are not satisfactory, it is a desirable type of TMM given its stability, reproducibility and low-cost.

### Beeswax

From Table 2, the  $\rho$  of the beeswax 0.96 g/cc has a variation of 7.96% (refer to Table 3) when compared to the reference value in Table 1. The beeswax CT image in Fig. 5b shows a few air-pockets in the sample. This image however, mimics the liver CT image presented in Fig. 5d. Although the

**Table 3** Experimental results of acoustic properties in the samples and their deviation compared to the reference Table 1

| Sample            | $\rho$ (g/cm <sup>3</sup> ) |             | $c_{us}$ (m/s) |             | AI (MRayls)    |             | $\mu$ (dB/MHz/cm) |
|-------------------|-----------------------------|-------------|----------------|-------------|----------------|-------------|-------------------|
|                   | Observed value              | % deviation | Observed value | % deviation | Observed Value | % deviation | Observed Value    |
| Polychloroprene50 | 1.45                        | 39          | 1706 ± 6.2     | 9.29        | 2.47           | 51.5        | 1.80 ± 0.02       |
| Beeswax           | 0.96                        | − 7.96      | 2323 ± 2.5     | 48.81       | 2.23           | 36.8        | 1.53 ± 0.01       |
| C-gel             | 1.03                        | − 1.25      | 1567 ± 4.4     | 0.38        | 1.61           | − 1.23      | 0.73 ± 0.01       |

The measured density ( $\rho$ ) (Eclipse<sup>TM</sup> system), the velocity of ultrasound ( $c_{us}$ ), acoustic impedance (AI), and attenuation coefficient ( $\mu$ ) are presented for the characterization of the acoustic properties of the samples. The percentage deviation of these results from the values of soft tissue in Table 1 is given. The results of the  $c_{us}$  and  $\mu$  are averages of ten measurements. The uncertainty in measurement of  $c_{us}$  is 0.05% (polychloroprene-50), 0.10% (beeswax), and 0.28% (C-gel) while the uncertainty in measurement of  $\mu$  is 1.05% (polychloroprene-50), 0.7% (beeswax), and 1.8% (C-gel). The measurement error for each sample is also mentioned

A negative value is obtained for results that are lower than the benchmark value



water-well is visible in the CT scan, the beeswax is primarily anechoic in the US image as shown in Fig. 5f. As pointed out in the case of polychloroprene, the scattering in beeswax may be inadequate to form an US image. The measured  $c_{us}$  in beeswax (2323 m/s) is higher than our requirement and the calculated AI given in Table 3, is higher by 36.8% from the benchmark. The higher AI is a result of higher  $c_{us}$  since the  $\rho$  of beeswax is acceptable.

The value of  $\mu$  in beeswax 1.53 dB/cm/MHz is unacceptable. Furthermore, the present beeswax does not satisfy the conditions of US imaging to mimic the US images of the liver and its acoustic properties also present a large deviation from soft-tissue. Since, the required conditions of imaging and acoustic properties are not satisfied, we find beeswax unsuitable for the intended application.

Waxes are low-cost, stable, and simple systems that can be easily moulded into desired shapes. In an attempt to reduce  $c_{us}$  in wax, investigators have explored materials like paraffin-gel wax, olefin polymers in mineral oil, and polyurethane gel for their tissue-mimicking properties for US [24–26]. In future work, the gel-wax system will be evaluated for similar applications.

### Carbomer gel

The  $\rho$  (1.03 g/cm<sup>3</sup>) of the *C-gel* compared to the reference value in Table 1, is within 2% (1.3% refer to Table 3) and is acceptable. In Fig. 5c, the CT image of *C-gel* shows a homogeneous sample that has a similar image contrast as the liver CT in Fig. 5d. The US image of the gel (shown in Fig. 5g) has speckle patterns similar to the US of liver (refer to Fig. 5h). The present *C-gel* is a homogenous medium where the individual scatterers exist too close, to be resolved by the US signal. In other words, the scatterers are separated by a distance smaller than the wavelength of the US wave that produce weak echoes appearing as a uniform complex mottled pattern (speckle) from the continuous scattering in the US image. The resultant  $c_{us}$  (1567 m/s) and the calculated AI (1.61 MRays) vary by 0.38% and 1.2% respectively in *C-gel*, refer to Table 3. However, the measured value of  $\mu$  (0.73 dB/cm/MHz) does not lie within the acceptable range. It is crucial for the value of  $\mu$  to be within 0.5–0.7 dB/cm/MHz to ensure the loss of US energy while travelling through a TMM and in soft-tissue is similar. We find this value higher by 4.3% from the upper acceptable limit of this parameter (0.7 dB/cm/MHz). This will cause the US to penetrate relatively less in the *C-gel* than in soft-tissue. However, from the speckle pattern it is confirmed that this will not affect its use as a TMM. The present results of *C-gel* satisfy the image criteria and the acoustic property closer to soft-tissue than the polychloroprene-50 and beeswax. Therefore, the present findings suggest that the *C-gel* can represent soft-tissue for US. The surface of a phantom

prepared using *C-gel* will not be firm to hold a transducer in place during a scan and this problem shall be addressed. Sealing the topmost surface of a *C-gel* phantom with a cling-film, will allow scanning with a transducer. Although, this phantom will not have a firm surface, the US imaging will be practically possible. Another, solution can be obtained using gel-wax. The gel-wax is a paraffin gel derived from high molecular weight saturated aliphatic hydrocarbons obtained from crude petroleum. It has been used recently in some US phantom studies [24]. Melted gel-wax can be poured over *C-gel* phantom. When left overnight the gel-wax sets into a firm surface. A small prototype phantom using *C-gel* and gel-wax was tested and this was found to generate images similar to soft-tissue scans.

The present results establish that imaging of the *C-gel* produces a uniform soft-tissue background in the CT and US images. These scans show contrast and echo-texture similar to the liver images; refer to the bottom two images in Fig. 5 in both the columns. The present gel prepared at 26 °C is highly viscous and non-drip. Moreover, this low-cost gel is physically stable under normal room conditions, free from microbial infestation, and is easy to prepare. Thus, the *C-gel* can provide a practical solution in making a low-cost TMM for the US that can be renewed in any clinical set-up, and hence can be widely employed in similar applications.

### Conclusions

In the present study CT, acoustic and ultrasonographic characterization of polychloroprene-50, beeswax and *C-gel* systems were performed to determine their ability to mimic soft-tissue for US. This required measuring their acoustic properties (a set of parameters). The results were compared with reference values derived from ICRU Report-61. Secondly, the CT and US images of these materials were compared to the contrast and echo-texture of human liver scans. For each test sample, the experimental results of  $c_{us}$ ,  $\rho$ , AI, and  $\mu$  were in agreement with their respective CT and US scans. As in the case of polychloroprene, there was a significant difference among the acoustic parameters from the desired values, these results were unacceptable. Later, this was also confirmed from the images of the rubber sample. A rubber-based US phantom can last a lifetime with proper handling. Therefore, a rubber having acceptable acoustic property will be a desirable material. Although the  $\rho$  and CT image of the beeswax sample were satisfactory, its US images were anechoic. The  $\rho$ ,  $c_{us}$ , and AI in *C-gel* were very close to the reference values. The CT and US images of *C-gel* could closely mimic the contrast and echogenicity of the liver scans representing a soft-tissue background in both the images. These results demonstrate *C-gel* to achieve the requirements better than any other sample in this study.

Although the temporal stability of the present gel is not studied here, commercial carbomer-940 gels are known to have a shelf-life of 2 to 3 years. *C-gel* is a non-toxic material that is easy to prepare. Containing 95% water, this gel can be prepared by following its recipe and reproduced widely for similar applications. These attributes make this system highly desirable. The acoustic properties of *C-gel* have not been studied elsewhere, during the reporting of this work. From the present findings, we suggest *C-gel* can be used as a TMM for diagnostic US. A diagnostic US phantom based on *C-gel* can offer an alternative to costly phantoms that will allow diagnostic US facilities to incorporate a periodic quality assurance program. This will help in a consistent, reliable and error-free reporting of this highly popular diagnostic tool.

**Acknowledgements** We gratefully acknowledge Dr. Naveen P. Kumar, Regional Cancer Center, Thiruvananthapuram, Kerala (India) for performing the ultrasound scans. We are grateful to Prof. M.R. Sarathchandras, Sree Chitra Thirunal College of Engineering, Thiruvananthapuram, Kerala (India) for helpful discussions regarding the velocity measurements. We thank Vajra Rubber Products (P) Ltd. Trichur, Kerala (India) for preparing the polychloroprene for testing.

**Funding** This research did not receive any specific grant from funding agencies in the public, commercial, or not-for-profit sectors.

## Compliance with ethical standards

**Conflict of interest** The authors have no conflicts of interest to declare.

**Ethical approval** This study was approved by the Institutional Scientific Review Committee.

**Informed consent** An informed consent of the patient was taken for using the diagnostic images in this study.

## References

- Bude RO, Adler RS (1995) An easily made, low-cost, tissue-like ultrasound phantom material. *J Clin Ultrasound* 23:271–273
- Annon LOMC, Agan ANJF, Rowne JAEB (2011) Novel tissue mimicking materials for high frequency breast ultrasound phantoms. *J Clin Ultrasound* 37:122–135. <https://doi.org/10.1016/j.ultrasmedbio.2010.10.005>
- Earle M, De PG, Devos E (2016) African federation for emergency medicine African journal of emergency medicine agar ultrasound phantoms for low-cost training without refrigeration Fanto`mes d`e `chographie utilisant l`agar-agar pour une formation a` faible cou`t, sans re`frige`ration. *Afr J Emerg Med* 6:18–23. <https://doi.org/10.1016/j.afjem.2015.09.003>
- Madsen EL, Frank GR, Dong F (1998) Liquid or solid ultrasonically tissue-mimicking materials with very low scatter. *Ultrasound Med Biol* 24:535–542. [https://doi.org/10.1016/S0301-5629\(98\)00013-1](https://doi.org/10.1016/S0301-5629(98)00013-1)
- Rowne JEB, Amnarine KVR, Atson AJW, Oskins PRH (2003) Original contribution assessment of the acoustic properties of common tissue- mimicking test phantoms. *Ultrasound Med Biol* 29:1053–1060. [https://doi.org/10.1016/S0301-5629\(03\)00053-X](https://doi.org/10.1016/S0301-5629(03)00053-X)
- Committee ATS (1990) Standard methods for measuring performance of pulse-echo ultrasound imaging equipment: American Institute of Ultrasound in Medicine Standard. AIUM, Laurel
- Goodsitt MM, Carson PL, Witt S, Hykes DL, Kofler JM (1998) Real-time B-mode ultrasound quality control test procedures: report of AAPM ultrasound task group no. 1. *Med Phys* 25:1385–1406. <https://doi.org/10.1118/1.598404>
- Garu PK, Chaki TK (2012) Acoustic & mechanical properties of neoprene rubber for encapsulation of underwater transducers. *Int J Sci Eng Technol* 237:231–237
- ASTM D2240-03 (2003) Standard test method for rubber property-Durometer hardness. <https://www.astm.org/DATABASE.CART/HISTORICAL/D2240-03.htm>. Accessed 13 Aug 2020
- Islam MT, Rodriguez-Hornedo N, Ciotti S, Ackermann C (2004) Rheological characterization of topical carbomer gels neutralized to different pH. *Pharm Res* 21:1192–1199
- Zhu W, Guo C, Yu A, Gao Y, Cao F, Zhai G (2009) Microemulsion-based hydrogel formulation of penciclovir for topical delivery. *Int J Pharm* 378:152–158
- Bushberg JT, Boone JM (2011) The essential physics of medical imaging. Lippincott Williams & Wilkins, Philadelphia
- Hendee WR, Ritenour ER (2003) Medical imaging physics. Wiley, Hoboken
- Mast TD (2000) Empirical relationships between acoustic parameters in human soft tissues. *Acoust Res Lett Online* 1:37–42. <https://doi.org/10.1121/1.1336896>
- International Commission on Radiation and Measurements ICRU (1998) Tissue substitutes, phantoms and computational modelling in medical ultrasound. ICRU
- Cameron J (1991) Physical properties of tissue. A comprehensive reference book, edited by Francis A. Duck. *Med Phys* 18:834
- Testing RF, Procedure T, Bude R, Adler RS, Metcalfe BSC, Evans JA et al (2010) A review of tissue substitutes for ultrasound imaging. *Ultrasound Med Biol* 15:1053–1060. <https://doi.org/10.1088/0031-9155/60/21/L23>
- de Kock EA, Schreuder AN, Schneider U (1996) The calibration of CT Hounsfield units for radiotherapy treatment planning. *Phys Med Biol* 41:1524–1527. <https://doi.org/10.1088/0031-9155/41/1/009>
- Cozzi L, Fogliata A, Buffa F, Bieri S (1998) Dosimetric impact of computed tomography calibration on a commercial treatment planning system for external radiation therapy. *Radiother Oncol* 48:335–338. [https://doi.org/10.1016/S0167-8140\(98\)00072-3](https://doi.org/10.1016/S0167-8140(98)00072-3)
- Huang J, Nissen JA, Bodegom E (1992) Diffraction of light by a focused ultrasonic wave. *J Appl Phys* 71:70–75
- Suheshkumar Singh M (2006) Ultrasound assisted optical tomography for characterization of optical and mechanical properties of soft biological tissues. Indian Institute of Science (IISc), Bangalore
- [https://www.nde-ed.org/GeneralResources/MaterialProperties/UT/ut\\_matlprop\\_metals.htm](https://www.nde-ed.org/GeneralResources/MaterialProperties/UT/ut_matlprop_metals.htm) n.d. Accessed 6 June 2020
- Capps RN (2005) Influence of carbon black fillers on acoustic properties of polychloroprene (neoprene) elastomers. *J Acoust Soc Am* 78:406–413. <https://doi.org/10.1121/1.392462>
- Maneas E, Xia W, Nikitichev DI, Daher B, Manimaran M, Wong RYJ et al (2018) Anatomically realistic ultrasound phantoms using gel wax with 3D printed moulds. *Phys Med Biol* 63:aa9e2c. <https://doi.org/10.1088/1361-6560/aa9e2c>
- Vieira SL, Pavan TZ, Junior JE, Carneiro AAO (2013) Paraffin-gel tissue-mimicking material for ultrasound-guided needle biopsy phantom. *Ultrasound Med Biol* 39:2477–2484. <https://doi.org/10.1016/j.ultrasmedbio.2013.06.008>

26. Oudry J, Bastard C, Miette V, Willinger R, Sandrin L (2009) Copolymer-in-oil phantom materials for elastography. *Ultrasound Med Biol* 35:1185–1197. <https://doi.org/10.1016/j.ultrasmedbio.2009.01.012>

**Publisher's Note** Springer Nature remains neutral with regard to jurisdictional claims in published maps and institutional affiliations.